THE EXPERIMENT
INTERNATIONAL JOURNAL OF SCIENCE AND TECHNOLOGY

ISSN-2319-2119

RESEARCH ARTICLE

S. Manouchehri et al, The *Experiment, 2014, Vol.26 (3)1816-1823*

REFRACTIVE INDEX, OPTICAL BANDGAP AND OSCILLATOR PARAMETERS OF PBS THIN FILMS DEPOSITED BY CBD TECHNIQUE

ABSTRACT

Nanocrystalline lead sulfide (PbS) thin films were synthesized on glass substrate by chemical bath deposition method using the solutions of lead nitrite, thiourea and sodium hydroxide. X-ray diffraction analysis revealed that thin films are single phase and have fcc structure. The average crystallite sizes were calculated using Scherrer's formula and are found to be about 41 nm and 47 nm depend on their thicknesses. The optical absorption, transmission and reflection were measured as a function of wavelength in the range of 300-950 nm. The optical band gaps of the samples are found to be 1.55 eV and 1.59 eV which are higher than the bulk one (0.41 eV). The dispersion of the refractive index is discussed in terms of the Wemple–DiDomenico single-oscillator model. The refractive index dispersion and oscillator parameters (oscillator energy, dispersion energy and oscillator strength) were calculated. The surface morphology studied using a scanning electron microscopy and showed that the films have uniform surface morphology over the entire substrate and were of good quality.

Keyword: nanocrystalline, lead sulfide, chemical bath deposition, optical band gap, oscillator parameter

1. INTRODUCTION

Lead sulfide (PbS) has attracted considerable attention owing to its especially small direct band gap (0.41 eV) and a larger excitation Bohr radius of 18 nm [1]. It is important in electronic and optoelectronic devices, infrared photography and photo thermal conversion applications [2]. The absorption edge has been found to be Red shifted as the particle size increased [3]. Polycrystalline PbS thin films showed good photoconductive properties [4]. These properties have been correlated with the synthesis method, thickness, composition and structure [5].

Both ''wet'' and ''dry'' methods of deposition have been used to form PbS thin films. Vacuum evaporation and molecular-beam epitaxy are among the most successful ''dry'' methods for PbS film synthesis. The frequently used ''wet'' methods include spray pyrolysis, chemical bath deposition and electrochemical deposition [6]. The chemical bath deposition (CBD) is the most used method to synthesize PbS films, Because it is a low cost method, easy to handle, and allows large area deposition of highly homogeneous films [7]. By CBD method, the dimensions of the crystallites can be controlled by varying the deposition parameters: reaction time, temperature, pH and presence of impurities in the solution [8].

In our present study, we utilized CBD method for growing PbS thin films at room temperature under atmosphere pressure. The optical properties were measured and the relative parameters were calculated. The dispersion of the refractive index is discussed in terms of the Wemple–DiDomenico single-oscillator model. The films thicknesses were measured by an optical interferometer.

2. Experimental

PbS thin films were grown on ordinary glass slide substrates by CBD technique. The deposition bath contained a mixture of aqueous solutions of lead nitrate, thiourea and sodium hydroxide in molar ratio 1:2:3 (mol/l) with volume proportion 2:2:3, respectively (all raw materials were from Merck Co. with purity higher than 99%). To have good quality thin films, cleaning of the substrate surface is very important. So the substrates were previously degreased in nitric acid and then cleaned in an ultrasonic cleaner with tripled distilled water. The cleaned substrates were vertically dipped into a 100 ml beaker, containing the mixed solutions, for 120 min at constant room temperature. Thickness of deposited thin films varied depending on the location of them in the beaker. The thicknesses of the samples varied between 250 nm to 400 nm. Two samples were chosen with various thicknesses, 250 nm and 400 nm. These samples named PbS1 and PbS2, respectively. The reaction process for forming lead sulfide films is considered as follows [9]:

$$Pb(NO_3)_2 + 2NaOH \rightarrow Pb(OH)_2 + 2NaNO_3$$

$$Pb(OH)_2 + 4NaOH \rightarrow Na_4Pb(OH)_6$$

$$Na_4Pb(OH)_6 \rightarrow 4Na + HPbO_2^- + 3OH^- + H_2O$$

THE EXPERIMENT
INTERNATIONAL JOURNAL OF SCIENCE AND TECHNOLOGY

ISSN-2319-2119

RESEARCH ARTICLE

$$SC(NH_2)_2 + OH^- \rightarrow CH_2N_2 + H_2O + SH^-$$
$$HPbO_2^- + SH^- \rightarrow PbS + 2OH^-$$

After deposition, the films were cleaned by triple distilled water and then dried at room temperature. The deposited films were smooth, homogeneous, well adherent to the substrate with dark surface like mirror.

The X-ray diffraction patterns of the samples were recorded on a PAN analytical X'Pert Pro MPD X-ray diffraction with Cu-Kα radiation (λ=1.5406 Å). The lattice parameters (a) for PbS thin films were calculated using below relation [10]:

$$d=a/(h^2+k^2+l^2)^{1/2} \quad (1)$$

Where h, k and l are the Miller indices; and d is the interplanar spacing. The average nanocrystallite size (D) was determined from the full width at half maximum (FWHM) of major diffraction peak using Scherrer's formula [11]:

$$D=0.9\lambda/\beta\cos\theta \quad (2)$$

Where λ is the X-ray wavelength (1.5406 Å), β is FWHM and θ is the diffraction angle.
SEM images were obtained on a Tescan scanning electron microscope (VEGA II). The UV–vis absorption was recorded on a UV–vis spectrophotometer (P70 UV-vis spectrometer PG Instrument Npd) in the range of 300-950 nm.

3. RESULTS AND DISCUSSION

3.1. XRD and SEM

Fig. 1 shows the XRD pattern of the nanocrystalline PbS1 and PbS2 thin films deposited at room temperature. All the diffraction peaks can be indexed to a face-centered-cubic (fcc) rock-salt structure of PbS according to the standard X-ray diffraction data file with reference No.77-0244. The absence of any other diffraction peaks indicates that there is no other crystalline phase. It can be easily inferred according to relative intensity from Fig. 1, there is a preferred orientation growth along the (200) diffraction peak.

The lattice parameter for PbS films was calculated by equation 1. It is found that the lattice constant is about 5.935±0.004 Å, which have a good congruence with standard lattice parameter data file with reference No.77-0244 (5.931 Å).The average crystallite sizes were calculated by equation 2 approximately 41 nm for PbS1 and 47 nm for PbS2.
Fig. 2 shows SEM images of the surface morphology of nanocrystalline PbS thin films. The thin films have uniform surface over the entire glass substrate and were of good quality. The estimated average grain sizes from SEM were about 100 nm for PbS1 and 110 nm for PbS2. Each of grains may be considered as the aggregation of a few smaller nanocrystallites and hence their size was found to be greater than that calculated from XRD measurements.

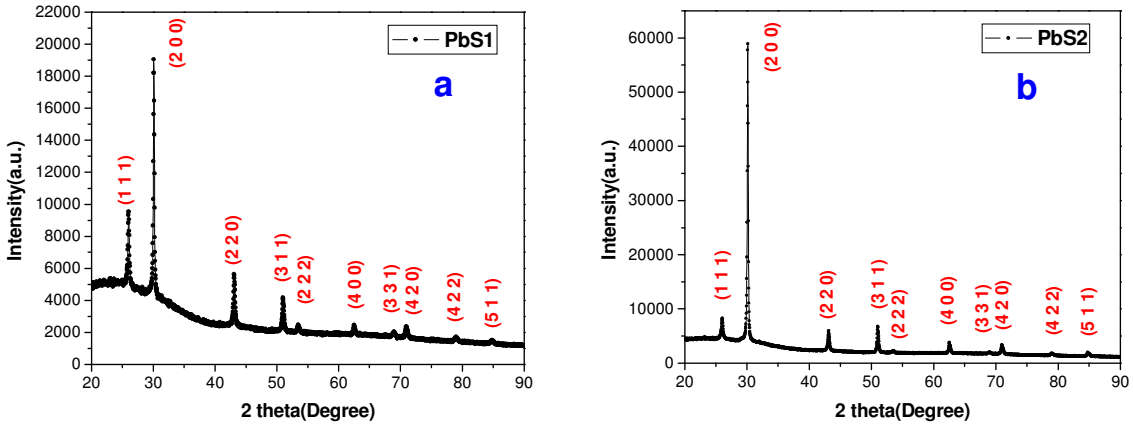

Fig. l: XRD patterns of (a) PbS1 and (b) PbS2 thin films.

THE EXPERIMENT
INTERNATIONAL JOURNAL OF SCIENCE AND TECHNOLOGY

ISSN-2319-2119

RESEARCH ARTICLE

S. Manouchehri et al, The *Experiment, 2014, Vol.26 (3)1816-1823*

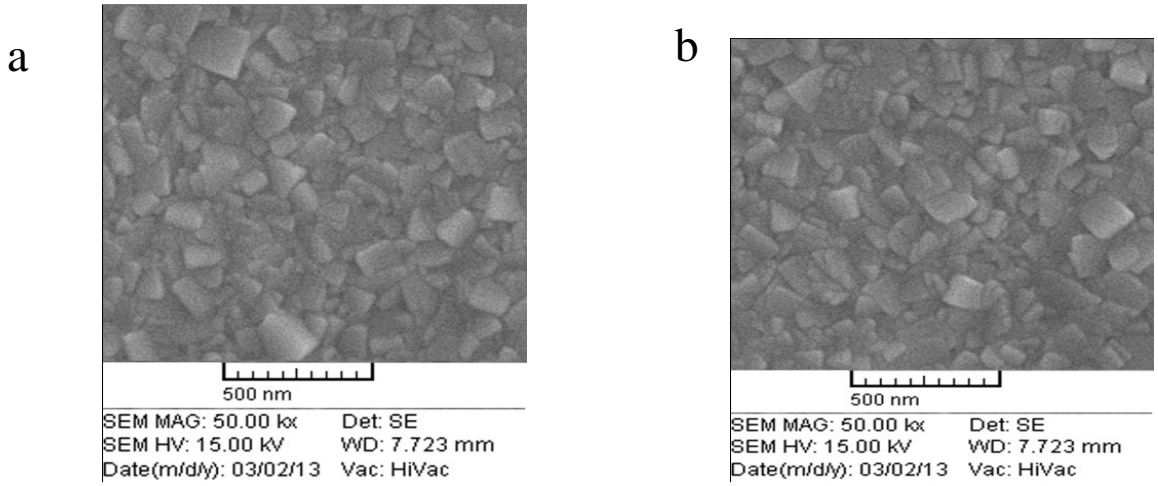

Fig. 2: SEM images of the surface morphology of (a) PbS1 and (b) PbS2 thin films.

3.2. Optical properties

The study of optical absorption is important means of determining the band structures, absorption coefficient (α) and energy band gap (E_g) of semiconductors. The action spectra were taken in the range of 300–950 nm.

Fig. 3 shows the UV-vis absorption spectra of PbS thin films with different thicknesses. The absorption spectrums of PbS thin films reveal an absorption common peak at 330 nm, a valley at 361 nm, absorption edges at 465 nm and 470 nm, and shoulders at 680 nm and 700 nm for PbS1 and PbS2, respectively. So, it is obvious that, the absorption edges and shoulders are slightly red-shifted by increasing the thickness of thin films, because the particle size increased and also, interference effects take place in long wave length portion of the spectra by increasing the thickness. These peaks correspond to exciton transition. The films have low absorption on the longer wavelength region.

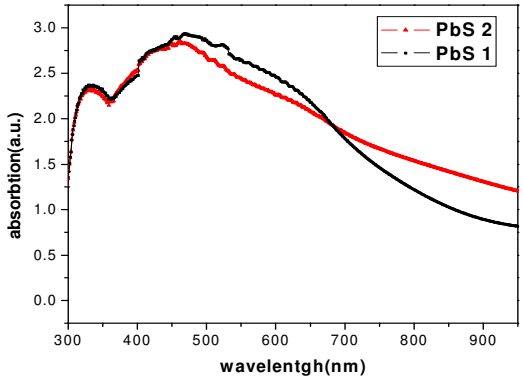

Fig. 3: The absorption spectra of PbS films

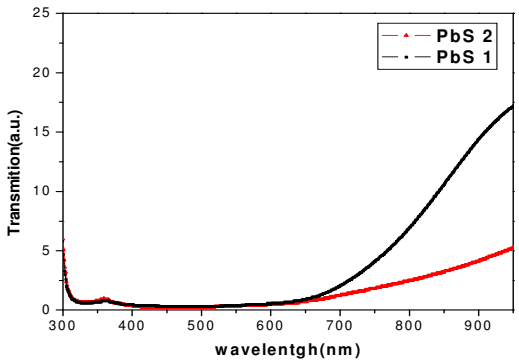

Fig. 4: The transmittance spectra of PbS films.

Fig. 4 shows the UV-vis transmittance spectrum of the samples. The transmittance of films is low for wavelength smaller than 600 nm, but there is a ramp on 361 nm which is due to the absorbance area of the films in this region. The transmittance increased by increasing wavelength towards the NIR regions. It can be seen from figure 3 and 4 that, the absorption and transmission of the samples are

THE EXPERIMENT
INTERNATIONAL JOURNAL OF SCIENCE AND TECHNOLOGY

ISSN-2319-2119

RESEARCH ARTICLE

S. Manouchehri et al, The *Experiment, 2014, Vol.26 (3)1816-1823*

compatible.

Fig. 5 shows the reflectance spectra of the samples. It is observed that the reflection behavior of films tends to reduction with increasing the wavelength. The reflectance spectra of films can be separated into three regions. In the first area up to 350 nm, there is a peak at about 330 nm which is corresponding to decreasing in the transmission and increasing the absorption. In second area up to 550 nm, there is a shoulder about 470 nm which is corresponding to the edge of absorption.

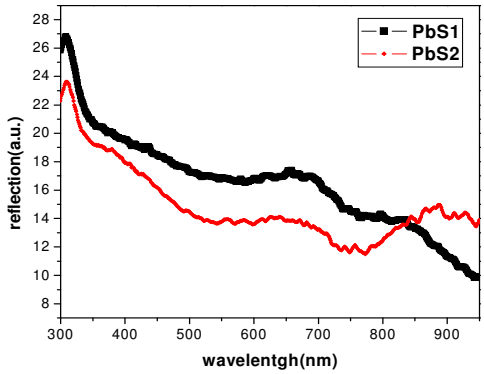

Fig. 5: reflectance spectra of PbS thin films.

At last, in third area for wavelength larger than 550 nm, it can be seen a ramp about 670 nm which is due to the shoulder of absorption spectra. The relation between the absorption coefficient 'α' and the incident photon energy '$h\nu$' for allowed direct type of transitions from Tauc's model can be written as [12]:

$$\alpha h\nu = A(h\nu - E_g)^{1/2} \quad (3)$$

where E_g is the band gap energy, ν is the frequency of the incident photon, h is the Planck's constant and A is a constant.
Fig. 6 shows $(\alpha h\nu)^2$ versus $(h\nu)$ for calculation the optical band gap. The optical band gap has been determined by extrapolation of the linear regions of the curve on '$h\nu$' axis. The straight line nature of the plots over a wide range of photon energy suggested allowed direct type of transition. It was found that the optical band gap to be about 1.6 eV and 1.55 eV for samples PbS1 and PbS2 respectively, which is higher than the bulk one (0.41 eV). So, it can be use as Optoelectronic devices [13, 14].

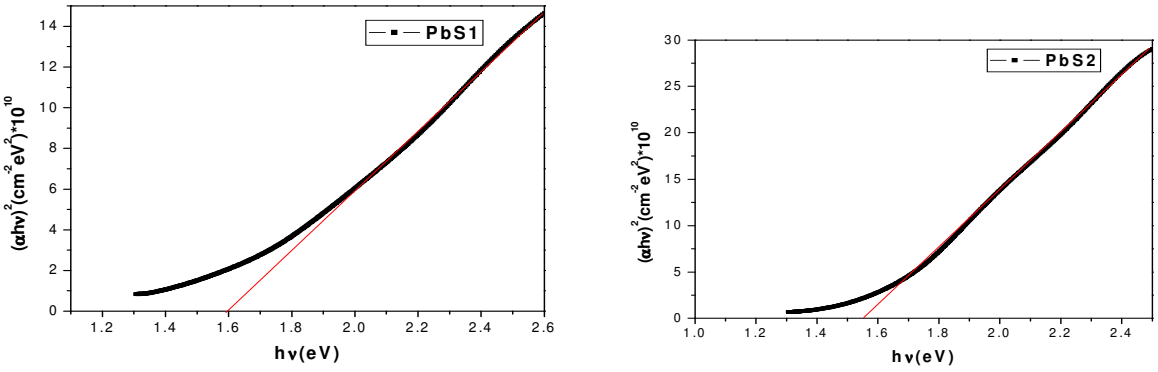

Fig. 6: The variation of $(\alpha h\nu)^2$ versus $(h\nu)$ for the samples.

3.3. Extinction coefficient

The extinction coefficient 'k' was calculated from the absorption coefficient using the classical relation [15]:

$$k = \alpha\lambda/4\pi \quad (4)$$

THE EXPERIMENT
INTERNATIONAL JOURNAL OF SCIENCE AND TECHNOLOGY

ISSN-2319-2119

RESEARCH ARTICLE

S. Manouchehri et al, The *Experiment, 2014, Vol.26 (3)1816-1823*

where λ is the wavelength of the incident radiation. Fig.7 shows the 'k' variations of PbS thin film versus wavelength of the incident radiation. So, the extinction coefficients of PbS thin films was shown a maximum close to their absorption edges, as to be expected.

3.4. Refractive index and dispersion of the thin films

The real part of the refractive index (n) was calculated using equation 4 and below equation [16]:

$$n=(1+R)/(1-R)+[4R/(1-R)^2-k^2]^{1/2} \quad (5)$$

Fig. 8 shows the dispersion plots 'n' of PbS thin films. It is observed that the refraction behavior of films tends to reduction with increasing the wavelength. The 'n' value's have a maximum lower than absorption edge, and it can be seen that this maximum slightly red-shifted by increasing the thickness.

The dispersion plays an important role in the research for optical materials in designing optoelectronic devices [17]. Refractive index dispersion can be analyzed by the single oscillator (Wemple–Didomenico) model [18]:

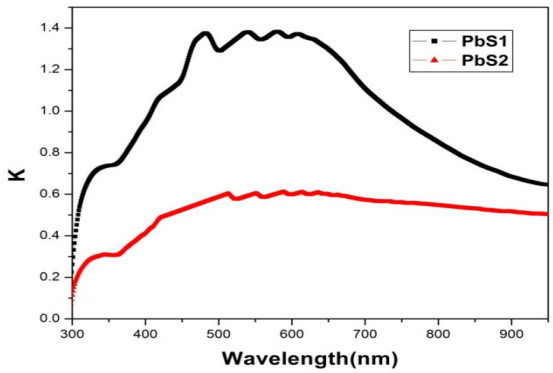

Fig. 7: The 'k' variations of PbS thin film versus the wavelength.

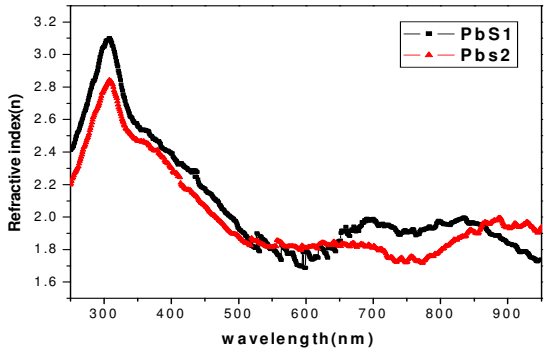

Fig. 8: The variation of 'n' relative to wavelength for PbS thin films.

$$n^2=1+E_0E_d/[E_0^2-(h\nu)^2] \quad (6)$$

where $h\nu$ is the photon energy, E_0 is the oscillator energy for electronic transitions and E_d is the dispersion energy, which is a scale of the strength of interband optical transitions. These parameters can be easily obtained by plotting of $(n^2\text{-}1)^{-1}$ versus $(h\nu)^2$ and Fig. 9 shows this plot for the samples. The values of E_d and E_0 listed in table 1, and it is obvious that by increasing the thickness, E_0 increased and E_d decreased.

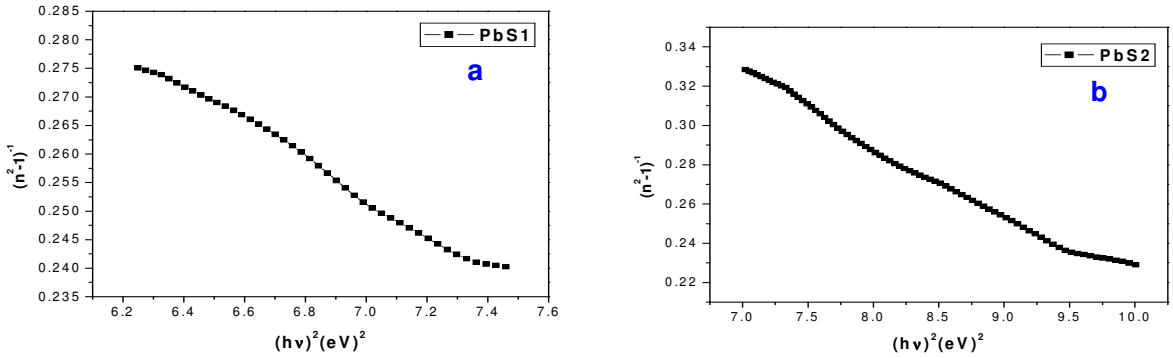

Fig.9: The plot of $(n^2\text{-}1)^{-1}$ versus $(h\nu)^2$ for (a) PbS1 (b) PbS2.

THE EXPERIMENT
INTERNATIONAL JOURNAL OF SCIENCE AND TECHNOLOGY

ISSN-2319-2119

RESEARCH ARTICLE

S. Manouchehri et al, The *Experiment, 2014, Vol.26 (3)1816-1823*

Table 1.Optical parameters of the synthesized PbS thin films.

Samples	E_g (eV)	E_0 (eV)	E_d (eV)	λ_0 (nm)	S_0 ($10^{13}m^{-2}$)	n_∞
PbS1	1.55	2.91	10.42	426	3.33	2.65
PbS2	1.6	3.03	7.99	410	3.12	2.49

The refractive index dependence on wavelength is expressed by the following dispersion relation [18]:

$$n^2-1=S_0\lambda_0^2/[1-(\lambda_0/\lambda)^2] \quad (7)$$

where λ is the wavelength of incident light, S_0 is the average oscillator strength and λ_0 is an average oscillator wavelength. The long wavelength refractive index (n_∞), average oscillator wavelength λ_0 and the average oscillator strength (S_0) for the thin films were determined using the following relationship [18]:

$$(n_\infty^2-1)/(n^2-1)=1-(\lambda_0/\lambda)^2 \quad (8)$$

The values of parameters n_∞, S_0, λ_0 were obtained from the plot of $(n^2-1)^{-1}$ versus λ^{-2}. The curves plotted and the results listed in Table 1. The energy E_0 is the average energy gap and it's scale with the Tauc gap E_g^{opt}, i.e. $E_0 \approx 2E_g^{opt}$, as it found by Tanaka [17]. The variation of parameters can be related to the thickness of films. These changes were shown that, the film thickness was suitable parameter for change the refractive index and oscillator parameters.

3. 5. Dielectric constant

The real part (ε_1) and imaginary part (ε_2) of the complex dielectric constant were calculated using the following formulas [19]:

$$\varepsilon_1=n^2-k^2 \quad (9a)$$

$$\varepsilon_2=2nk \quad (9b)$$

Fig. 10 shows the wavelength dependence of the real part of the complex dielectric constant for PbS thin films. As can be seen, the maximum values of ε_1 were reached in the low wavelength region.

Fig. 11 shows the wavelength dependence of the imaginary part of the complex dielectric constant. The behavior of ε_1 was similar to refractive index because of the smaller value of k^2 comparison of n^2, while ε_2 mainly depends on the values of k, which are related to the variation of absorption coefficient. It is seen that the real part of dielectric constant decreased by increasing wavelength and the values of real part is higher than imaginary part.

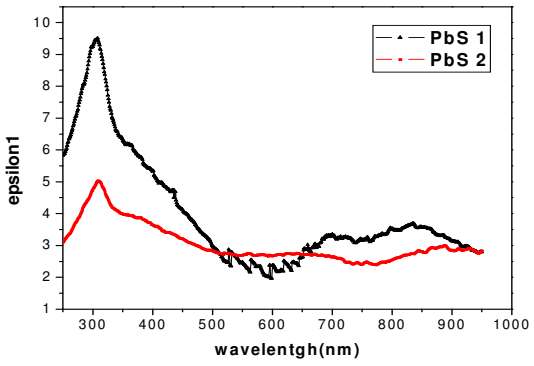

Fig. 10: The wavelength dependence of real part of dielectric constant.

THE EXPERIMENT
INTERNATIONAL JOURNAL OF SCIENCE AND TECHNOLOGY

ISSN-2319-2119

RESEARCH ARTICLE

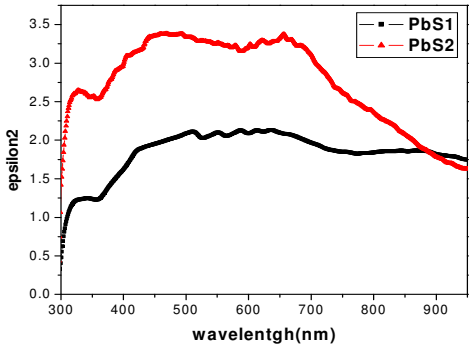

Figure 11: The wavelength dependence of imaginary part of dielectric constant for PbS1 and PbS2 .

4. CONCLUSIONS

Thin films of PbS1 and PbS2 were prepared on glass substrates at room temperature by CBD technique. From XRD and SEM, it can be deduced that the thin films were single phase and have a fcc structure and have good quality. The optical constants were determined from the transmittance and reflectance. It is found that the absorption, reflection and transmission of the samples are compatible, and the transmittance decreased by increasing the absorption. The absorption edge, refractive index and the dielectric constant of the films are influenced by the film thickness and wavelength. It was seen that the film thickness was suitable parameter for change the refractive index and oscillator parameters. Furthermore, the optical band gap values which calculated by W-D model and Tauc model were nearly the same. So we can use these thin films for optoelectronic devices in IR region.

REFERENCES

1. W. Wu, Y. He, Y. Wu, T. Wu, Self-template synthesis of PbS nanodendrites and its photocatalytic performance, J. Alloy. Compd. 509 (2011) 9356-9362.
2. K.C. Preetha, K.V. Murali, A.J. Ragina, K. Deepa, T.L. Remadevi, Effect of cationic precursor pH on optical and transport properties of SILAR deposited nano crystalline PbS thin films, Curr. Appl. Phys. 12 (2012) 53-59.
3. N. Choudhary, B.K. Shrma, Structural characterization of nanocrystalline PbS thin films synthesized by CBD method, Indian J. Pure. Ap. Phy. 46 (2008) 261-265.
4. R. Kumar, P. Kumar-Sahu, R. Das , S. Tiwari, Synthesis and Structural Properties of Nanocrystalline $(Pb_{1-x}Bi_x)S$ Thin Films, Adv. Phys. Theories Appl. 19 (2013) 101-104.
5. V. Popescu, G.L. Popescu, M. Moldovan, C. Perjmerean , Photosensitization of PbS films by thermal treatment in controlled environment, Chalcogenide Lett. 6 (2009) 503-508.
6. P. Thirumoorthy , K.R. Murali, Characteristics of pulse electrodeposited PbS thin films, J. Mater. Sci.-mater. El. 22 (2011) 72-76.
7. L. Raniero, C.L. Ferreira, L.R. Cruz, A.L. Pinto, R.M.P. Alves, Photoconductivity activation in PbS thin films grown at room temperature by chemical bath deposition, Physica B 405 (2010) 1283–1286.
8. M.M. Abbas, A. Ab-M. Shehab, N-A. Hassan, A-K. Al-Samuraee, Effect of temperature and deposition time on the optical properties of chemically deposited nanostructure PbS thin films, Thin Solid Films 519 (2011) 4917–4922.
9. S. Seghaier, N. Kamoun, R. Brini, A.B. Amara, Structural and optical properties of PbS thin films deposited by chemical bath deposition, Mater. Chem. Phys. 97 (2006) 71–80.
10. S. Kumar, T.P. Sharma, M. Zulfequar, M. Husain, Characterization of vacuum evaporated PbS thin films, Physica B 325 (2003) 8–16.
11. M. Mozafari, F. Moztarzadeh, D. Vashaee, L. Tayeb, Effects of heat treatment on physical, microstructural and optical characteristics of PbS luminescent nanocrystals, Physica E 44 (2012) 1429–1435.
12. M.A. Barote, S.S. Kamble, A.A. Yadav, E.U. Masumdar, Optical and electrical characterization of chemical bath deposited Cd–Pb–S thin films, Thin Solid Films 526 (2012) 97-102.

13. S. Kaci, A. Keffous, M. Trari, H. Menari, A. Manseri, B. Mahmoudi, L. Guerbous, Influence of polyethylene glycol-300 addition on nanostructured lead sulfide thin films properties, Opt. Commun. 283 (2010) 3355–3360.
14. N.F. Borillie, D.W. Smith, Quantum confiment of PbS microstructure in glass, J. Non-Cryst. Solids 180 (1994) 25-31.
15. N. K. Reddy, K.T.R. Reddy, Optical behaviour of sprayed tin sulphide thin films, Mater. Res. Bull. 41 (2006) 414–422.
16. S. Ilican, Y. Caglar, M. Caglar, F.ahrettin, Y.Caglar, M. Caglar, Optical characterization of the $CdZn(S_{1-x}Se_x)$ thin films deposited by spray method, J. Alloy. Compd. 480 (2009) 234–237.
17. Z.Z. You, G.J. Hua, Refractive index, optical band gap and oscillator parameters of organic films deposited by vacuum evaporation technique, Vacuum 83 (2009) 984–988.
18. K. Goksen, N.M. Gasanly, Refractive index, oscillator parameters and temperature-tuned energy band gap of $Ti_4In_3GaS_8$- layered single crystals, J. Phys. Chem. Solids 69 (2008) 2385‑ 2389.
19. F. Yakuphanoglu, A. Cukurovali, I. Yilmaz, Single-oscillator model and determination of optical constants of some optical thin film materials, Physica B 353 (2004) 210–216.

S. Manouchehri*, J. Zahmatkesh, M. Heidari-Sani, T. Barzekar, M.H. Yousefi

*Department of physics, Malek-Ashtar University of Technology,
Shahinshahr, Esfahan 83145-34177, Iran.